A Novel Identification Algorithm for Rotor Initial Angle in Double-Fed Wind Power Generator

Yuan LI

School of Electrical and Photo Electronic Engineering, Changzhou Institute of Technology,

Changzhou，Jiangsu，213002，China;

***Abstract* — In double-fed wind power generation system, the AC voltage amplitude, frequency and angle should be controlled to meet the relevant parameters of the grid. The main contact can be closed when errors between parameters of stator and grid are within a certain range. There is an initial angle between rotor and stator when the generator is still. Therefore, this angle should be identified and used in the vector control algorithm. To solve this problem, a method of the rotor initial angle identification by PI controllers is proposed, which is simple and effective to improve dynamic performance and reduce the cutting-in current. The method proposed is derived in detail, and verified using Matlab/Simulink simulation experiments and prototype testing. Both simulation and experimental studies prove that the proposed method is correct and effective.**

Keywords - Doubly-fed motor, Wind power, Parameter identification, Vector control

I. INTRODUCTION

Doubly-fed induction motor (DFIM), which means both the motor stator windings and rotor windings can be connected to AC power (bidirectional feed), is generally adopted wound rotor induction motor structure. Doubly-fed motor speed control system with adjustable power factor, high efficiency, small capacity inverter device, investment, etc., there is a vast market and development prospects [1].

f_1 and f_2 are defined as DFIM stator and rotor AC power frequency respectively. n_1 is the stator magnetic field rotational speed, i.e. synchronous speed; n_2 is the rotor magnetic field relative to the rotor speed; n_r is DFIM rotor speed. It can be obtained by the knowledge of electro-mechanics, when DFIM operating stably, that $n_1=n_r+n_2$. Due to $f_1=n_1/60$ and $f_2=n_2/60$, there is $n_r/60+f_2=f_1$. From the above equation, when the generator speed changes, by adjusting the rotor excitation current frequency to keep the stator frequency is constant, which is the principle of variable speed constant frequency (VSCF) operation. Generator running in sub-synchronous state, $f_2> 0$, the rotor and the stator winding is the same phase sequence; When the generator is running at super- synchronous state, $f_2 <0$, the rotor and the stator is the reverse phase sequence; When the generator is running at synchronous state, $f_2 =0$, the rotor is DC excited.

From the above analysis, in the case of wind speed changes, the main function of the machine side converter is operating in VSCF state, tracking the giver power, feeding power to the grid. Since the mathematical model is different when stator is connected to the grid or not, the machine side converter control strategies can be divided into: the cutting-in control strategies and the connected control strategies. In order to achieve synchronization with the line-voltage vector for soft connection to the line grid, the information (amplitude, frequency and phase) about line voltages is also needed. Double-fed wind power generation system, especially in the megawatt level applications, the cutting-in control strategies play a crucial role to the whole system [2-5].In terms of traditional asynchronous wind turbines control system, there will be 5 to 7 times or 10 times the impact of current without the cutting-in control strategies [6].In the double-fed wind generator control, how to control the stator voltage by using rotor current, it is the key to tracing grid voltage and cutting-in grid. Currently, conventional cutting-in control strategies includes the stator voltage open-loop control and the stator voltage closed-loop control [7]. The former can be divided into the rotor current open loop control strategy and the rotor current closed-loop control strategy. The latter can also be divided into the stator voltage RMS loop control strategy and the instantaneous value of the stator voltage closed-loop control strategy.

In this paper, based on the instantaneous value of the stator voltage closed-loop control strategy, we propose a method of the rotor initial angle identification, and applied to vector control, which can effectively reduce the impact of the current and improve dynamic performance when connecting to the gird.

II. MATHEMATIC MODELING OF THE DFIM

Under assumption of linear magnetic circuits and balanced operating condition, the equivalent two-phase model of the symmetrical DFIM with stator connected to line, represented in fixed stator d-q reference frame is (1) [8-10].

$$\begin{cases} \dfrac{\mathrm{d}\psi_{\mathrm{ds}}}{\mathrm{d}t} = \alpha L_{\mathrm{m}} i_{\mathrm{dr}} - \alpha\psi_{\mathrm{ds}} + \omega_{\mathrm{l}}\psi_{\mathrm{qs}} + U_{\mathrm{m}} \\ \dfrac{\mathrm{d}\psi_{\mathrm{qs}}}{\mathrm{d}t} = \alpha L_{\mathrm{m}} i_{\mathrm{qr}} - \alpha\psi_{\mathrm{qs}} - \omega_{\mathrm{l}}\psi_{\mathrm{ds}} \\ \dfrac{\mathrm{d}i_{\mathrm{dr}}}{\mathrm{d}t} = -\gamma i_{\mathrm{dr}} + \omega_{\mathrm{s}} i_{\mathrm{qr}} + \alpha\beta\psi_{\mathrm{ds}} - \beta\omega\psi_{\mathrm{qs}} - \beta U_{\mathrm{m}} + \dfrac{u_{\mathrm{dr}}}{L_{\mathrm{r}}\sigma} \\ \dfrac{\mathrm{d}i_{\mathrm{qr}}}{\mathrm{d}t} = -\gamma i_{\mathrm{qr}} - \omega_{\mathrm{s}} i_{\mathrm{dr}} + \alpha\beta\psi_{\mathrm{qs}} + \beta\omega\psi_{\mathrm{ds}} + \dfrac{u_{\mathrm{qr}}}{L_{\mathrm{r}}\sigma} \\ \dfrac{\mathrm{d}\omega}{\mathrm{d}t} = [\mu(\psi_{\mathrm{qs}} i_{\mathrm{dr}} - \psi_{\mathrm{ds}} i_{\mathrm{qr}}) - T_{\mathrm{L}}]/J \end{cases} \quad (1)$$

where *i, ψ, u, R ,L , L_m , U_m ,ω, $ω_s$,T_L* and *J* represent current, flux linkage, voltage, resistance, inductance, mutual inductance, stator terminal voltage, rotor electrical angular speed, slip electrical angular speed, external load torque and the moment of inertia respectively. The subscripts *s* and *r* stand for stator and rotor while subscripts *d* and *q* stand for vector component with respect to a fixed stator reference frame. $\sigma = 1 - L_m^2 / L_r L_s$ is the redefined leakage inductance. *α, β* and *μ* are defined as $\alpha = R_s/L_s$, $\beta = L_m/(L_s \cdot L_r \cdot \sigma)$ and $\mu = 3 \cdot np \cdot L_m/(2 \cdot L_s)$. n_p denotes number of pair of poles.

III. METHOD OF ROTOR INITIAL ANGLE IDENTIFICATION

A. Problem posing

In the double-fed motor control system, the rotor position and speed should be detected by using photoelectric encoder. However, when using the optical encoder to detect the rotor position, the initial position of the rotor cannot be detected.

Fig.1 shows in the *d-q* coordinate system between the phase angle between motor stator and rotor winding, which is represented by θ_r. When the DFIM operating in stationary state, the rotor angle θ_r is defined as θ_0.As can be seen from Fig.1, if θ_0 is not identified effectively, it will affect the vector control and the tracing control of stator. When the angle difference θ_0 is little, it can be used the d-axis voltage component error between stator and grid to correct based on instantaneous voltage closed-loop control. However, when the difference is large, it is difficult to be corrected. The angle θ_0 must be compensated and computed in vector control by using the angle identification method.

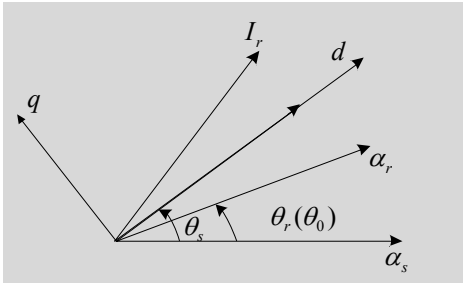

Figure 1. The Vector Figure of Double-fed Induction Motor

B. Principle of rotor initial angle identification

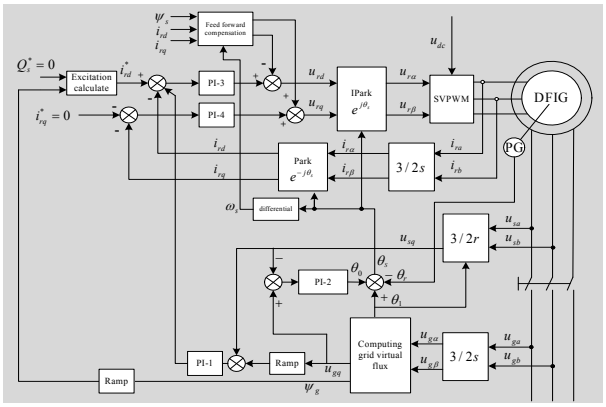

Figure 2. The Vector Figure of Double-fed Induction Motor

In the paper, the method rotor initial angle identification is proposed, which using the voltage q-axis component error between stator and the grid to identify the θ_0, showed as Figure 2 [1].

As can be seen from the figure, by using the initial angle identification, the compensation can be calculated and rotor current q-axis component can be set to zero directly. The actual slip angle θ, can be calculated by the θ_1、 θ_r and θ_0. In this paper, the conventional PI controller is used to construct the identifier (Figure 2 .PI-2).

C. Principle of identification based on PI

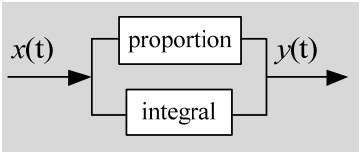

Figure 3. Block Diagram of PI Control Principle

Parameter identification principle based on PI control algorithm is shown in Figure 3 [11-13]. *x* (t)& *y*(t) are input and output of the identification algorithm and K_P&K_I are the proportional, integral factor of the PI control algorithm.

$$y(t) = K_P\left[x(t) + \frac{1}{K_I}\int_0^t x(t)dt\right] \quad (2)$$

Set the sampling time Δ*t*, after the ceremony discrete:

$$y(k) = K_P\left[x(k) + \frac{1}{K_I}\Delta t_s\sum_0^k x(k)\right] \quad (3)$$

Case 1：The measured input values for several sampling time unchanged, namely: $x(k) = x(k-1) = x(k-2) = \cdots$

Then:

$$y(k) = K_P\left[x(k) + \frac{1}{K_I}\Delta t_s\sum_0^k x(k)\right] = K_P\left[x(k-1) + \frac{1}{K_I}\Delta t_s\sum_0^{k-1} x(k-1)\right] + \frac{K_P}{K_I}x(k)\Delta t_s \quad (4)$$

$$y(k-1)=K_P\left[x(k-1)+\frac{1}{K_I}\Delta t_s\sum_0^{k-1}x(k-1)\right] \quad (5)$$

Equation 4 minus equation 5:

$$y(k)-y(k-1)=\frac{K_P}{K_I}x(k)\Delta t_s \quad (6)$$

set $\alpha=\dfrac{y(k)-y(k-1)}{x(k)\Delta t_s}$, $K_{PI}=\dfrac{K_P}{K_I}$, then:

$$K_{PI}=\frac{K_P}{K_I}=\frac{y(k)-y(k-1)}{x(k)\Delta t_s}=\alpha \quad (7)$$

Case 2: When two consecutive measuring input value is 0 and the subsequent measured input and output are $x(j)$、$y(j)$:

$$y(j-1)=K_P\left[x(j-1)+\frac{1}{K_I}\Delta t_s\sum_0^{j-1}x(j-1)\right]= \quad (8)$$
$$\frac{K_P}{K_I}\Delta t_s\sum_0^{j-1}x(j-1)$$

$$y(j)=K_P\left[x(j)+\frac{1}{K_I}\Delta t_s\sum_0^{j}x(j)\right]= \quad (9)$$
$$K_Px(j)+\frac{K_P}{K_I}\Delta t_s\sum_0^{j-1}x(j-1)+\frac{K_P}{K_I}x(j)\Delta t_s$$

Equation 8 minus equation 9 and set $b=\dfrac{y(j)-y(j-1)}{x(j)}$, then:

$$K_P\left(1+\frac{1}{K_I}\Delta t_s\right)=\frac{y(j)-y(j-1)}{x(j)}=b \quad (10)$$

From equation 6 minus equation 9:

$$K_P=b-\alpha\Delta t_s \quad (11)$$

$$K_{PI}=K_P/K_I=\alpha \quad (12)$$

From equation 11 minus equation 12, the parameter can be identified, so these two equations above can be used to identify the initial angle of the rotor.

IV. SIMULATION EXPERIMENT

In this paper a simulation experiment and a 1.5MW prototype experiment are used to verify the effectiveness of the proposed control strategy, the simulation and prototype motor parameters is shown in Table 1.

TABLE I. PARAMETERS OF 1.5MW DFIG

Rated voltage U	**Rated power P**	**Pair of poles p**
690(V)	1500(kW)	2
Stator resistance	**Rotor resistance**	**Stator inductance**
0.0035(Ω)	0.0084(Ω)	0.0495(mH)
Rotor inductance	**Mutual inductance**	**Rated speed**
0.0415(mH)	0.0088(mH)	1800(r/min)

In Figure 4, the stator voltage output is controlled by a ramp and the channel information is shown below:

CH1: Voltage of grid phase A;

CH2: Voltage of motor stator phase A.

Figure 4(a) is the waveform of stator voltage tracking gird voltage without amplitude control and without compensation of initial rotor angle (PI-1&PI-2 in Figure 2 are not used). As it is shown in the figure, rotor voltage and gird voltage have a huge deviation and cannot satisfy the requirement of grid-connection.

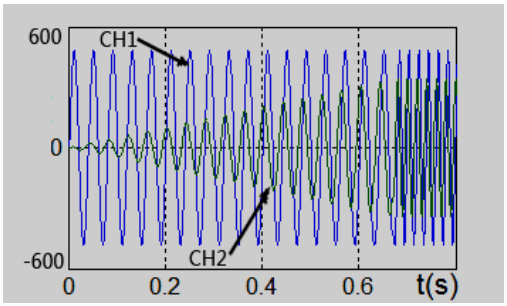

(a) No amplitude control and no compensation of θ_0

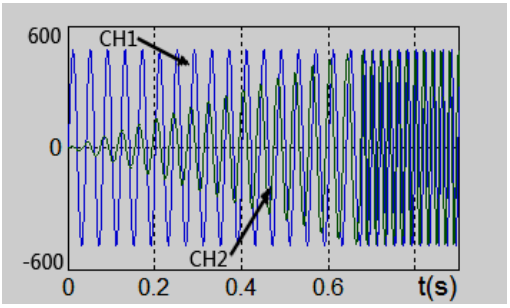

(b) With amplitude control and no compensation of θ_0

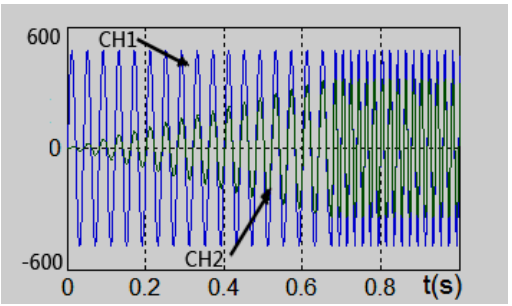

(c) With compensation of θ_0 and no amplitude control

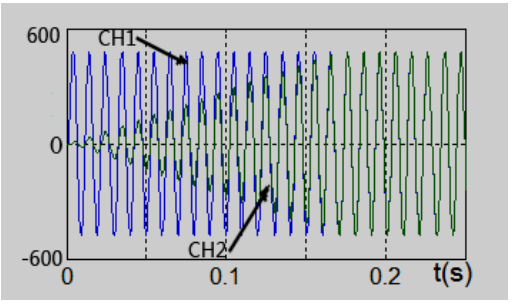

(d) With compensation of θ_0 and amplitude control

Figure 4. Simulation Waveforms of Novel Grid Connection Strategy

Figure 4 (b) is the waveform of stator voltage tracking gird voltage with amplitude control but without compensation of initial rotor angle (PI-1 is used but PI-2 is not used). As it is shown in the figure, the amplitude of rotor voltage and gird voltage can be tracked but they have a phase shift.

Figure 4 (c) is the waveform of stator voltage tracking gird voltage without amplitude control but with compensation of initial rotor angle (PI-1 is not used but PI-2 is used). As it is shown in the figure, the amplitude of rotor voltage and gird voltage cannot be tracked but they have no phase shift.

Figure 4 (d) is the waveform of stator voltage tracking gird voltage with amplitude control and compensation of initial rotor angle (PI-1&PI-2 are all used). As it is shown in the figure, the amplitude and of rotor voltage and gird voltage can be tracked and they have no phase shift.

V. PROTOTYPE EXPERIMENT

Experiment system is made up by a 2MW squirrel-cage induction motor as prime motor and a 1.5MW doubly-fed induction motor as generator. The experiment system is shown in Figure 5(a) below. The converters for prime motor and generator are shown in Figure 5 (b).

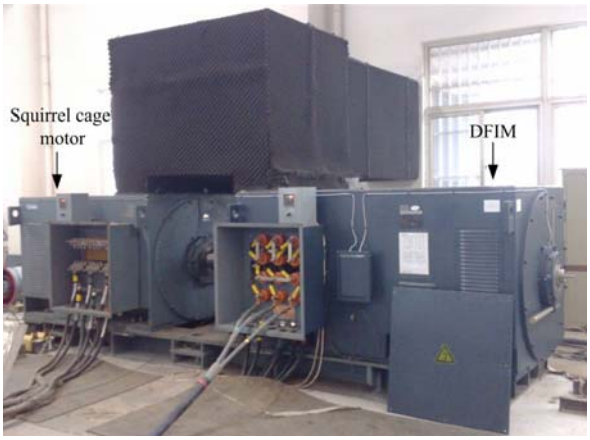

(a) Experimental motors platform

(b) Experimental converters

Figure 5. Experimental motors platform

In Figure 6, the oscilloscope channel information is shown below:

CH1: Line voltage of stator A and B(50V/div);
CH2: Line voltage of gird A and B (100V/div);
CH3: Stator current of phase A (100A/div);
CH4: Rotor current of phase A (100A/div).

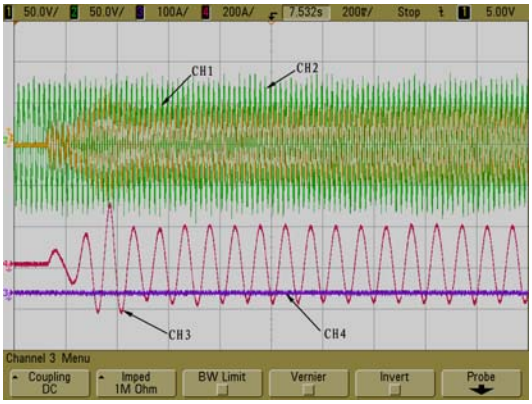

(a) No amplitude control and no compensation of θ_0

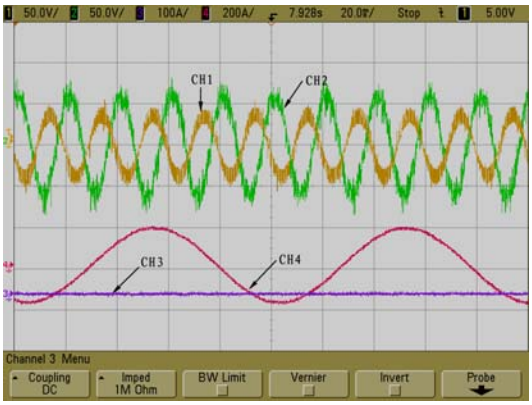

(b) No amplitude control and no compensation of θ_0 in detail

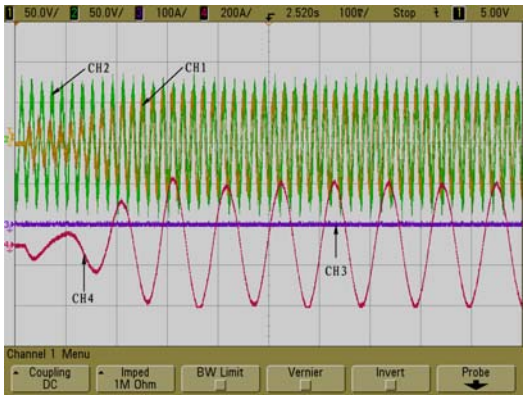

(c) With amplitude control and no compensation of θ_0

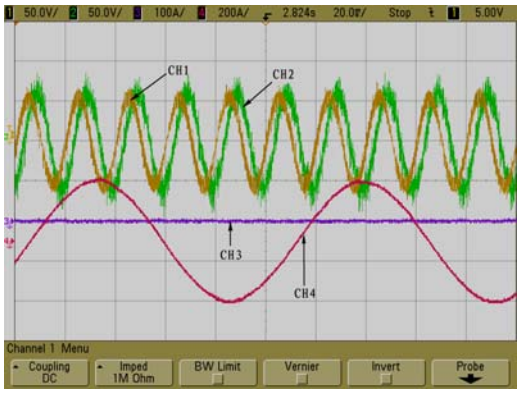

(d) With amplitude control and no compensation of θ_0 in detail

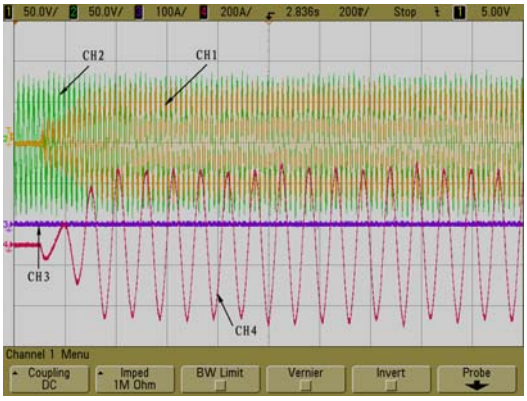

(e) With compensation of θ_0 and amplitude control

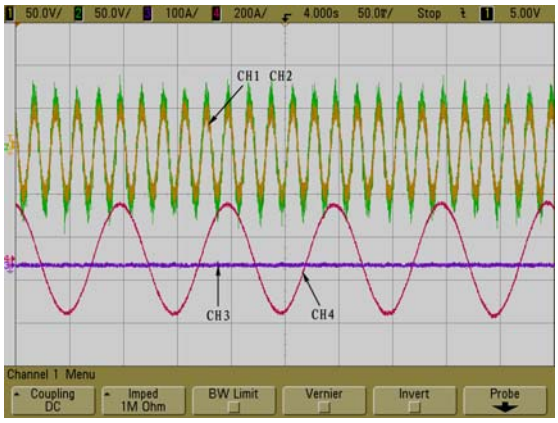

(f) With compensation of θ_0 and amplitude control in detail

Figure 6. Waveform of tracking voltage control

Figure 6 (a) & (b) are the waveforms of stator voltage tracking gird voltage without amplitude control and without compensation of initial rotor angle.

As it is shown in the figure, rotor voltage and gird voltage have a huge deviation and cannot satisfy the requirement of grid-connection.

Figure 6(c) & (d) are the waveforms of stator voltage tracking gird voltage with amplitude control but without compensation of initial rotor angle. As it is shown in the figure, the amplitude of rotor voltage and gird voltage can be tracked but they have a phase shift, so the grid-connection cannot be satisfied too.

Figure 6(e) & (f) are the waveforms of stator voltage tracking gird voltage with amplitude control and compensation of initial rotor angle. As it is shown in the figure, the amplitude and of rotor voltage and gird voltage can be tracked and they have no phase shift, so the grid-connection can be satisfied within 1 second.

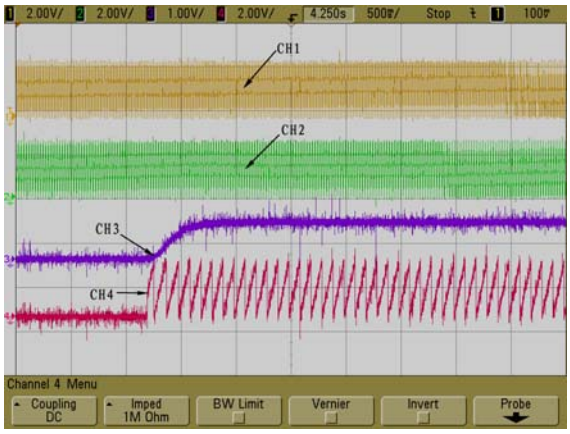

(a) Relevant angle waveform

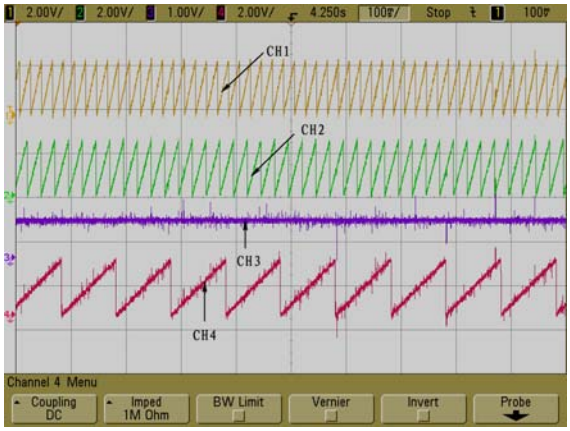

(b) Relevant angle waveform in detail

Figure 7. Related angle waveform

Figure.7 shows the waveform of initial rotor angle identification before grid connected. CH1 is virtual grid flux angle, CH2 is the rotor angle, CH3 is the compensation angle and CH4 is the slip angle. As shown in the figure the identification is accurate and the identification speed is about 300ms.

VI. CONCLUSIONS

In this paper, the problem of the rotor initial angle in the process of double-fed wind power generation system grid connection is proposed firstly. The deviation of q-axis component of stator voltage and grid voltage and a PI

controller is used for the identification of rotor initial angle. The angle is applied to stator voltage instantaneous value control strategy. The simulation and experiment results shown the improvement of the performance of the stator voltage tracking and the correctness and effectiveness of the proposed control strategy is verified.

REFERENCES

[1] Y. Li, Key Technology Research of Megawatt Three-level Double-fed Wind Power Converter[D].Xu Zhou : China University of Mining and Technology.

[2] Q. H . Liu,Y. K. He,S. J. Bian, "Study on the No-Load Cutting-in Control of the Variable-Speed Constant-Frequency(VSCF) Wind-Power Generator," Proceedings of the CSEE, 24(3),pp.6-11,2004.

[3] Q. H . Liu,Y. K. He,J. H. Zhang,"Grid Connection Control Strategy of AC-excited Variable-speed Constant-frequency Wind Power Generator," Automation of Electric Power Systems,30(3), pp.51-55,2006.

[4] S. Y. Meng,S. J. Xie," Design of the Grid Connection Controller for Wind Turbine Asynchronous Generator Based on DSP," Electric Switchgear.41(6),pp.27-30,2003.

[5] R. Pena, J. C. Clare, G. M. Asher,"Doubly fed induction generator using back-to-back PWM converters and its application to variable-speed wind-energy generation," IEEE Proc. Electr. Power Applications,1996,143(3):231-241.

[6] M. Tavakoli Bina, E. Pashajavid. "An efficient procedure to design passive LCL-filters for active power filters," Electric Power Systems Research,79,pp.606-614,2009.

[7] E. J. Bueno, F. Espinosa, J. Francisco, " Current Control of Voltage Source Converters connected to the grid through an LCL-filter," Annual IEEE Power Electronics Specialists Conference,35,pp.68-73,2004.

[8] S. Peresada,A. Tilli,A. Tonielli,"Power control of a doubly fed induction machine via output feedback," Control Engineering Practice,12(1),pp.41-57,2004.

[9] S. Peresada,A. Tilli,A. Tonielli,"Indirect stator flux-oriented output feedback control of a doubly fed induction machine," IEEE Transaction on Control Systems Technology,11(6), pp.875-888, 2003.

[10] S. Drid, M. Tadjine,M. S. Naït-Saïd,"Robust backstepping vector control for the doubly fed induction motor," IET Control Theory Appl,1(4),pp.861-868,2007.

[11] Y. F. Zhang,Y. Yuan,S. P. Hao,"Parameter identification of digital PI controller and experiment validation," Electric Power Automation Equipment,30(11),pp.40-43, 2010.

[12] M. G. Zhang,W. H. Li,M. Q. Liu,"Adaptive PID Control Strategy Based on RBF Neural Network Identification," International Conference on Neural Networks and Brain, Beijing,China:IEEE,2005,pp.1854-1857.

D. S. Pereira,J. O. P. Pinto,"Genetic algorithm based system identification and PID tuning for optimum adaptive control," Proceedings,2005 IEEE/ASME International Conference on Advanced Intelligent Mechatronics.Long Beach,CA,USA:IEEE, 2005,pp.801-806.